Journal of Neuroscience Research 86:2932–2942 (2008)

Signaling Pathways of Bisphenol A–Induced Apoptosis in Hippocampal Neuronal Cells: Role of Calcium-Induced Reactive Oxygen Species, Mitogen-Activated Protein Kinases, and Nuclear Factor–κB

Soyoung Lee,[1] Kyoungho Suk,[1] In Kyeom Kim,[1] Il-Sung Jang,[2] Jin-Woo Park,[3] Victor J. Johnson,[4] Taeg Kyu Kwon,[5] Byung-Ju Choi,[2] and Sang-Hyun Kim[1]★

[1]CMRI, Department of Pharmacology, School of Medicine, Kyungpook National University, Daegu, Republic of Korea
[2]Department of Pharmacology, School of Dentistry, Kyungpook National University, Daegu, Republic of Korea
[3]Department of Periodontology, School of Dentistry, Kyungpook National University, Daegu, Republic of Korea
[4]Toxicology and Molecular Biology Branch, Biostatistics Branch, Health Effects Laboratory Division, NIOSH, Morgantown, West Virginia
[5]Department of Immunology, School of Medicine, Keimyung University, Daegu, Republic of Korea

In the present study, we investigated the neurotoxicity of bisphenol A [BPA; 2,2-bis-(4 hydroxyphenyl) propane] and the underlying mechanisms of action in mouse hippocampal HT-22 cells. BPA, known to be a xenoestrogen, is used in the production of water bottles, cans, and teeth suture materials. BPA-treated HT-22 cells showed lower cell viability than did controls at concentrations of BPA over 100 μM. BPA induced apoptotic cell death as indicated by staining with Hoechst 33258, costaining with Annexin V/propidium iodide, and activation of caspase 3. BPA regulated the generation of reactive oxygen species (ROS) by increasing intracellular calcium. BPA activated phosphorylation of extracellular signal–regulated kinase (ERK) and *c-Jun* N-terminal kinase (JNK), and nuclear translocation of nuclear factor (NF)-κB. Pretreatment with specific inhibitors for calcium, ROS, ERK, and JNK decreased BPA-induced cell death; however, inhibitor for NF-κB increased BPA-induced cell death. The results suggest that calcium, ROS, ERK, and JNK are involved in BPA-induced apoptotic cell death in HT-22 cells. In contrast, an NF-κB cascade was activated for survival signaling after BPA treatment.

Key words: bisphenol A; apoptosis; reactive oxygen species; nuclear factor-κB; mitogen-activated protein kinase

Bisphenol A [BPA; 2,2-bis-(4 hydroxyphenyl) propane], a monomer in polycarbonate plastics and a constituent of epoxy, has been used extensively in the food-packaging industry (Staples et al., 1998). Because of an increase in the use of products based on BPA, the possibility of environmental contamination by BPA has increased. Recent studies have shown that routes of human exposure to BPA were identified in water, air, and soil environment, and food contamination including can surfaces and plastic containers (Tsai, 2006). BPA released from polycarbonate flasks during autoclaving was also shown to have estrogenic effects (Staples et al., 1998). However, BPA has been reported to have not only estrogenic activity but also several other types of biological toxicity. BPA induces apoptosis in several types of cells, including primary germ and sertoli cells (Hughes et al., 2000; Oka et al., 2003). BPA has potent harmful effects on multipotent neural progenitor cells through altered mitogen-activated protein kinase (MAPK) signaling and reactive oxygen species (ROS) generation (Kim et al., 2007a). However, little is known about the specific mechanisms of BPA's neurotoxic effects.

Contract grant sponsor: Korea Science and Engineering Foundation (KOSEF) grant funded by the Korea government (MOST); Contract grant number: M10646020001-06N4602-00110; Contract grant sponsor: Basic Research Program; Contract grant number: R01-2005-000-10103-0.

★Correspondence to: Sang-Hyun Kim, Department of Pharmacology, Kyungpook National University Medical School, 101 Dong-In, Joong-gu, Daegu, 700-422, Republic of Korea. E-mail: shkim72@knu.ac.kr

Received 17 December 2007; Revised 26 February 2008; Accepted 29 February 2008

Published online 2 June 2008 in Wiley InterScience (www.interscience.wiley.com). DOI: 10.1002/jnr.21739

ROS induce undesirable biological reactions including cell death (Buttke and Sandstrom, 1994). Several studies have shown that BPA induces ROS generation and oxidative stress in rodent liver, sperm, and brain (Bindhumol et al., 2003; Chitra et al., 2003). BPA induces overproduction of ROS in mouse organs and Neuro2a cells in a time-dependent manner (Kabuto et al., 2003; Ooe et al., 2005). Moreover, it is widely known that transient Ca^{2+} fluxes lead to a lethal change in calcium homeostasis and increases in ROS and eventually induce cell death.

Several intracellular signal transduction cascades including MAPKs are known to play important roles in regulating cell growth, differentiation, and apoptosis. The major MAPKs are extracellular signal-regulated kinase (ERK), *c-Jun* N-terminal kinase (JNK), and p38. The MAPK family is known to be related to cellular toxic events such as neuronal cell death and differentiation (Purves et al., 2001). ERK was recently implicated in the regulation of neural stem cell fate (Hao et al., 2004). Oxidative stress induces activation of JNK and p38 via phosphorylation, which induces stress-mediated apoptotic signal (Ichijo et al., 1997).

A transcription factor, nuclear factor–κB (NF-κB), has important activity as a mediator of cellular responses to extracellular signals. NF-κB is an inducible and ubiquitously expressed transcription factor for genes involved in cell survival, differentiation, inflammation, and growth (Pande and Ramos, 2005). NF-κB is related to neurite formation, as well as the survival and death of neuronal cells (Foehr et al., 2000). Several studies have demonstrated that interference with differentiation of neuronal cells may be a critical factor in neuronal cell survival, and it is involved in differential activation of MAPK and NF-κB in TNF-α-induced cortical neuronal cell death and Zn-induced interference with differentiation of PC-12 cells (Seo et al., 2001; Sakon et al., 2003).

The effects of estrogenic-related activity of BPA on the developmental stage have been largely studied. However, the neurotoxic effects of BPA have not been elucidated despite the extensive use of BPA in various fields. In this study, the potential adverse effects of BPA on neuronal cell death were investigated using hippocampal cells. The objectives of this study were to define BPA-induced apoptotic cell death and the molecular neurotoxic mechanism of BPA. We hypothesized that the initial effects of BPA induced the mobilization of Ca^{2+} and subsequent generation of ROS. In turn, these effects activate pathways leading to apoptosis. We therefore investigated the possibility of whether intracellular Ca^{2+}, ROS, MAPKs, NF-κB, and caspases are implicated in BPA-induced apoptosis. The use of inhibitors at different stages confirmed the involvement of the respective molecules in signaling pathways.

MATERIALS AND METHODS

Materials and Cell Cultures

Bisphenol A was purchased from the Kasei Co. (Tokyo, Japan). The fluorescent probes propidium iodide (PI), Hoechst 33258 (H33258), Annexin V, Fluo-3/AM, dihydrorhodamine 123 (DHR), and BAPTA-AM were procured from Molecular Probes (Eugene, OR). Ethylene glycol–bis(β-aminoethyl ether)-tetra acetic acid (EGTA), *N*-acetyl-cysteine (NAC), and phorbol 12-myristate 13-acetate (PMA) were procured from Sigma Chemical Co. (St. Louis, MO). PD98059, SP600125, and pyrrolidine dithiocarbamate (PDTC) were purchased from Calbiochem-Novabiochem Corporation (La Jolla, CA). Mouse hippocampal cell lines (HT-22 cell) were grown in Dulbecco's minimum essential medium (DMEM) with 2 mM glutamine, 100 units/mL penicillin, and 100 μg/mL streptomycin and supplemented with 10% fetal bovine serum (GIBCO, Grand Island, NY) in 5% CO_2 at 37°C.

MTT Assay

Cell viability was determined using the 3(4,5-dimethyl thiazolyl-2)2,5-diphenyl tetrazoliumbromide (MTT) assay in 96-well plates as previously described (Kim et al., 2002). Cells (2×10^4 cells/well in 96-well plates) were treated with various concentrations of BPA for 24 hr followed by incubation with MTT for 4 hr, and then 100 μL of isopropanol (in 0.04N hydrochloric acid) was added to dissolve the formazan crystals. Absorbance was read at 570 nm using an Anthos 2010 spectrophotometer (Salzburg, Austria). Cell viability was calculated as relative absorbance compared with the control and expressed as percentage of the control.

Morphological Detection of Apoptosis and Necrosis

The fluorescent probes PI, H33258, and Annexin V were used according to the manufacturer's protocols to measure necrotic and apoptotic cell death. Briefly, cells (2×10^5cells/well in 12-well plates) were incubated with BPA for 4 or 8 hr. Following incubation, cells were stained with either PI (5 μg/mL in PBS), H33258 (10 μg/mL in PBS), or Annexin V [5 μL/100 μL in Annexin-binding buffer: 10 mM HEPES, 140 mM NaCl, 2.5 mM $CaCl_2$ (pH 7.4)] for 15 min. Fluorescence intensity for PI was detected at an excitation of 535 nm and emission of 617 nm, for H33258 at an excitation of 350 nm and emission of 450 nm, and for Annexin V at an excitation of 495 nm and emission of 520 nm. Costaining with Annexin V and PI was employed to detect apoptotic and necrotic cells in the same culture and visualized in a fluorescence microscope (Olympus BX51, Center Valley, PA) as indicated below.

Determination of Intracellular Ca^{2+}

Morphological evaluation of the cells was performed with a fluorescence microscope (Olympus BX51). To determine intracellular Ca^{2+}, Fluo-3/AM was used according to the manufacturer's protocol, a brief description of which follows. Cells (2×10^4cells/well in 96-well plates) were preincubated with Fluo-3/AM for 60 min. After washing the dye from the cell surface, BPA and EGTA were added for 20 min; then fluorescent intensity was photographed or recorded using a fluorescent plate reader (Fluostar OPTIMA, BMG LABTECH, Offenburg, Germany) at an excitation of 485 nm and emission of 520 nm and digitized.

ROS Generation

The production of ROS was measured by detecting the fluorescent intensity of the oxidant-sensitive probe dihydrorhodamine 123 (DHR). Cells (2×10^4 cells/well in 96-well plates) were washed with PBS, which was supplemented with 10 μM of DHR, and the intracellular and extracellular dye concentrations were allowed to equilibrate at 5% CO_2 at 37°C for 30 min. Iron ($FeSO_4$, 100 μM) was used as a positive control for ROS generation. All pharmacological agents (1.5 mM EGTA, 10 μM BAPTA) were added 30 min before the BPA treatment. The cells were then incubated with BPA, and the kinetics of fluorescent intensity for DHR was recorded using a fluorescent plate reader (Fluostar OPTIMA) at an excitation of 480 nm and emission of 525 nm. The fluorescent readings were digitized using Soft Max Pro (Molecular Devices, Sunnyvale, CA).

Nuclear Protein Extraction

Preparation of nuclear extract was basically as described elsewhere (Lee et al., 2007). Briefly, after cell activation with 400 μM BPA for the times indicated, cells (2×10^6 cells/well in 6-well plates) were washed in 1 mL of ice-cold PBS, resuspended and centrifuged at 400*g* for 5 min, resuspended in 100 μL of ice-cold hypotonic buffer [10 mM HEPES/KOH, 2 mM $MgCl_2$, 0.1 mM EDTA, 10 mM KCl, 1 mM DTT, 0.5 mM PMSF (pH 7.9)], left on ice for 10 min, vortexed, and centrifuged at 15,000*g* for 30 sec. Pelleted nuclei were gently resuspended in 20 μL of ice-cold saline buffer [50 mM HEPES/KOH, 50 mM KCl, 300 mM NaCl, 0.1 mM EDTA, 10% glycerol, 1 mM DTT, 0.5 mM PMSF (pH 7.9)], left on ice for 20 min, vortexed, and centrifuged at 15,000*g* for 5 min at 4°C. Aliquots of the supernatant that contained nuclear proteins were frozen in liquid nitrogen and stored at −70°C.

Western Blot Analyses

Cells (2×10^6 cells/well in 6-well plates) were treated with 400 μM BPA for the indicated time (within 120 min). Following treatment, cells were washed with PBS, and total cell lysates were prepared by scrapping in 100 μL of lysis buffer (20 mM Tris-HCl, 120 mM NaCl, 50 mM HEPES, 1% Triton-X, 1 mM EDTA, 2 mM sodium orthovanadate, 1 mM DTT, 10% glycerol, 0.02 mM PMSF, 1 mg/mL leupeptin, 1 mg/mL aprotinin). Samples of protein were electrophoresed using 8%–12% SDS-PAGE and then transferred to nitrocellulose membranes. The membranes were stained with the reversible Ponceau S to ascertain equal loading of samples in the gel. The caspase 3, p65 NF-κB, and IκBα were assayed using anti-pro–caspase 3, anti-NF-κB (p65), and anti-IκBα antibodies, respectively (Santa Cruz Biotech, Santa Cruz, CA). Activation of p38, JNK, and ERK was determined using anti-phospho-p38, -JNK, and -ERK antibodies, respectively (Cell Signaling, Beverly, MA). Immunodetection was performed using an enhanced chemiluminescence detection kit (Amersham Pharmacia, Piscataway, NJ).

Determining Early Apoptosis and Necrosis by Flow Cytometry

To further determine the presence of early apoptosis and necrosis, cell death was analyzed by staining cells with Annexin V and PI. For staining, cells (2×10^5 cells/well in 12-well plates) were treated with BPA and/or potent inhibitors. Cells were washed with PBS, centrifuged, and suspended in Annexin V–binding buffer containing 5 μL/100 μL of Annexin V and PI (final concentration 5 μg/mL) as provided by the manufacturer. The cells were incubated in a 5% CO_2 atmosphere at 37°C for 15 min and analyzed using a flow cytometer (BD Biosciences Pharmingen, San Diego, CA). The fluorochrome was excited using a line of an argon ion laser, and Annexin V and PI emissions were monitored at 525 and 620 nm, respectively. A total of at least 1×10^4 cells were analyzed per sample.

Transfection and Luciferase Assays

HT-22 cells (1×10^5 cells/well in 12-well plates) were plated 1 day before transient transfection with a NF-κB luciferase reporter gene construct (pNF-κB-LUC, a plasmid containing an NF-κB binding site; STANTAGEN, Grand Island, NY). Transfection was performed in serum- and antibiotic-free medium containing 4 μL of Lipofectamine 2000 reagent (Invitrogen, Carlsbad, CA). After 4 hr of incubation, the medium was replaced with DMEM medium containing 10% FBS and antibiotics. Cells were allowed to recover at 37°C for 20 hr. The cells were treated with BPA for 2 hr and then lysed. For luciferase activity assay, cell lysates were prepared and assayed for luciferase activity using the Luciferase Assay System (Promega, Madison, WI) according to the manufacturer's instructions.

Electrophoretic Mobility Shift Assays (EMSA)

Nuclear protein (10 μg) was incubated for 20 min at room temperature with 2 μg of poly(dI-dC) from Pharmacia (Uppsala, Sweden), 2 μL of buffer M [(20 mM HEPES/KOH, 20% glycerol, 100 mM KCl, 0.5 mM PMSF (pH 7.9)], 4 μL of buffer K [20% ficoll-400, 100 mM HEPES, 300 mM KCl, 10 mM DTT, 0.5 mM PMSF (pH 7.9)], and 20,000 cpm of a ^{32}P-labeled probe encoding the NF-κB consensus sequence (5′-GAT CTC AGA GGG GAC TTT CCG AGA AGA-3′) in a final volume of 20 μL of DNA–protein complex resolved at 120 V for 2 hr in a 5% polyacrylamide gel, dried, and exposed to X-ray film.

Statistical Analysis

Statistical analyses were performed using SAS statistical software (SAS Institute, Cary, NC). Treatment effects were analyzed using one-way analysis of variance, followed by Duncan's multiple-range tests. Significance was set at $P < 0.05$.

RESULTS

BPA-Induced Cytotoxicity in Hippocampal Cells

To study the cytotoxic effect of BPA, we employed the MTT assay (Fig. 1) as an indirect mea-

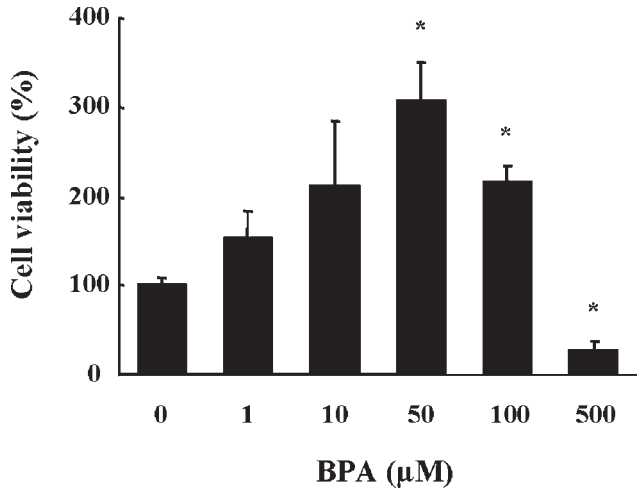

Fig. 1. Effects of BPA on cell viability in HT-22 cells. HT-22 cells (2×10^4 cells/well in 96-well plates) were treated with various concentrations of BPA for 24 hr. Cell viability was determined using the MTT assay. Cell viability is represented as relative absorbance compared to the control. The results are presented as means ± SEMs of three independent experiments (*significantly different from the control).

surement of cell viability. HT-22 cells were treated with various concentrations of BPA for 24 hr. HT-22 cells showed higher cell viability than did the control when the concentration of BPA was below 100 μM but lower cell viability when the concentration was greater than 100 μM. BPA induced apoptotic cell death when the concentration of BPA was greater than 100 μM. The viability of HT-22 cell exposed to 400 μM BPA for 24 hr was reduced to 57% of the control. For researching apoptosis, we treated HT-22 cells with 400 μM BPA in most experiments.

BPA-Induced Apoptosis

To elucidate the nature of cell death by BPA, we examined cell apoptosis using microscopy and flow cytometry. Cells were exposed to 400 μM BPA for 4 or 8 hr and stained with H33258. The morphology of cells is displayed fragmented nuclei by apoptosis (Fig. 2A). To differentiate the apoptotic cells and necrotic cells, we co-stained with Annexin V and PI, and simultaneously visualized both cells by overlaying (Fig. 2B). The apoptotic cells displayed green fluorescence with Annexin V staining, and the necrotic cells displayed red fluorescence

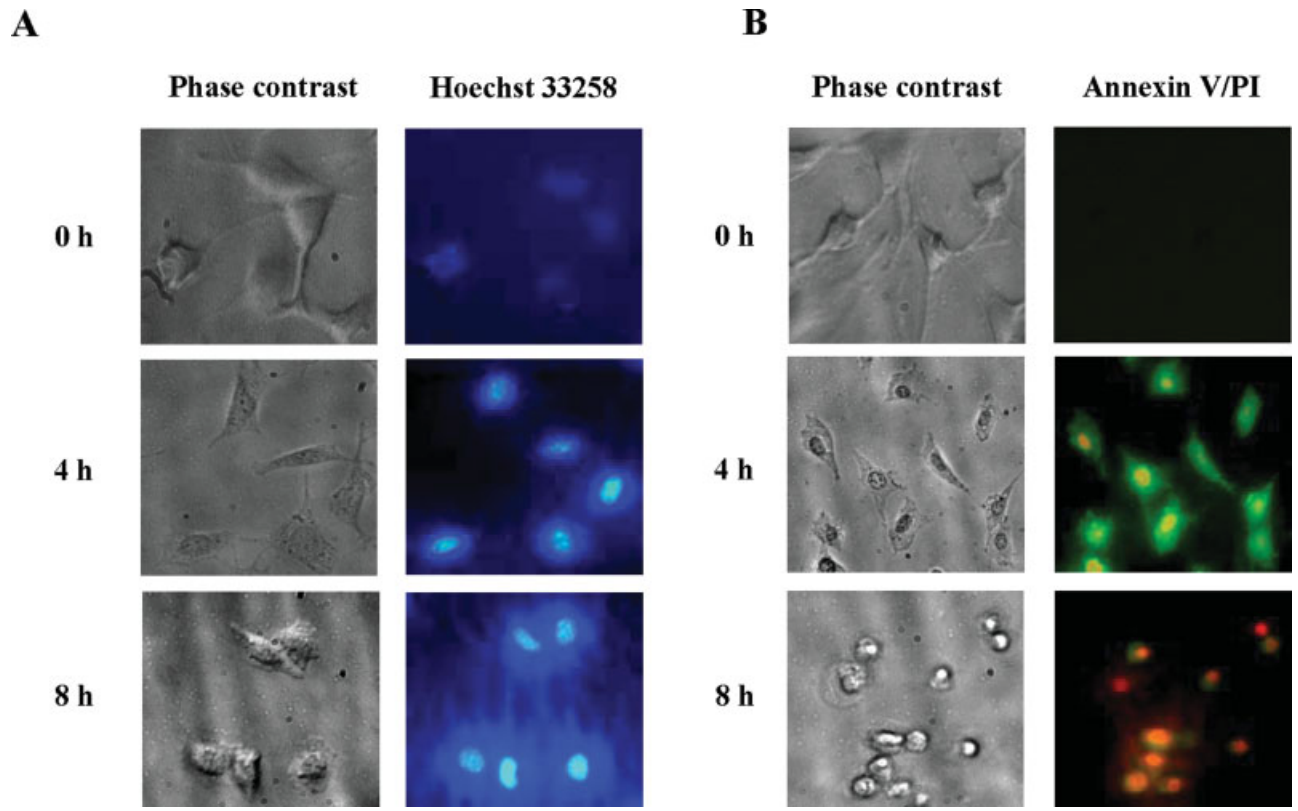

Fig. 2. Effects of BPA on cell death. **A:** Cells (2×10^5 cells/well in 12-well plates) were treated with 400 μM of BPA for 4 or 8 hr. After treatment with BPA, cells were stained with fluorescent probes. Cells were stained with H33258 and visualized by a fluorescence microscope. Representative photographs show a phase-contrast image and an image of H33258 for DNA fragmentation. **B:** For comparisons of BPA-induced apoptotic and necrotic cell death, cells treated with BPA for 4 or 8 hr were costained with Annexin V and PI, and fluorescence was visualized by a fluorescence microscope. Representative photographs show a phase-contrast image and a overlap image of Annexin V and PI for apoptosis and necrosis. Similar results were observed in three independent experiments. [Color figure can be viewed in the online issue, which is available at www.interscience.wiley.com.]

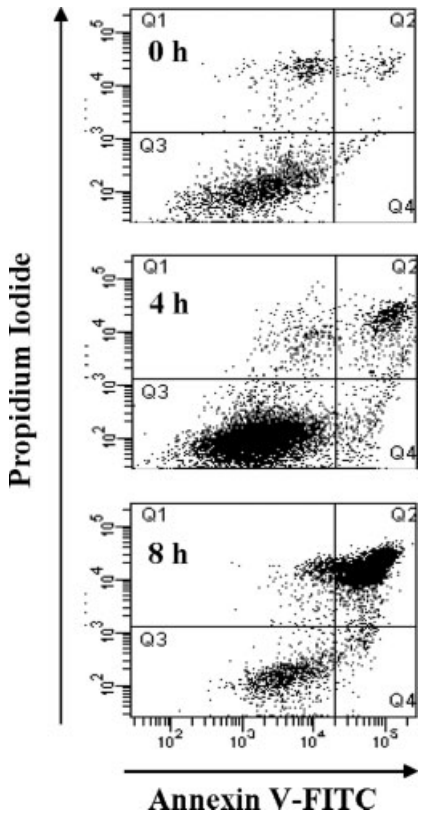

Fig. 3. Effect of BPA on apoptosis and necrosis. Cells (2×10^5 cells/well in 12-well plates) were treated with 400 μM of BPA for 4 or 8 hr, following which Annexin V binding was performed according to the Materials and Methods section. Live cells are in the lower left quadrant. The upper right quadrant represents necrotic and late apoptotic cells, and the lower right quadrant represents early apoptotic cells. Similar results were observed in three independent experiments.

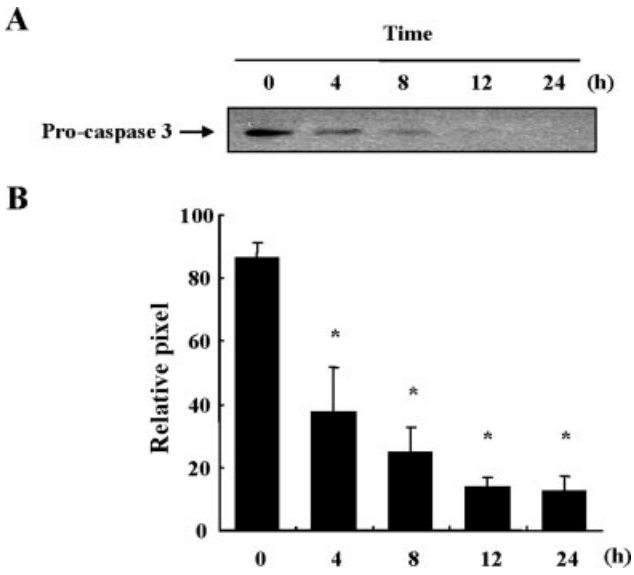

Fig. 4. Effects of BPA on caspase 3 activation. **A:** Cells (2×10^6 cells/well in 6-well plates) were treated with 400 μM of BPA at the indicated times, and the blots were examined with anti-pro–caspase 3 antibody. **B:** Densitometric analysis of pro–caspase 3. The results are presented as means ± SEMs of three independent experiments. (*significantly different from the control).

with PI staining. Cells treated with 400 μM BPA showed strong green fluorescence and weakly neuronal extension. Flow cytometry was used to confirm this result (Fig. 3). Live cells, displayed in the lower left quadrant of Figure 3, were negative for both stains. With Annexin V, the live cells showed little fluorescent stain, and the apoptotic cells displayed substantially higher fluorescence intensity in the green channel. The percentage of cells in the Annexin V-FITC area increased to 68.4% after 8 hr. Thus, the Annexin V binding assay confirmed cell death in HT-22 cells treated with BPA. To further evaluate apoptotic signaling by BPA, activation of caspase 3 was detected. Caspase 3 activation is an integral step in most apoptotic events. To examine whether caspase 3 was activated, we studied cleavage of pro–caspase 3. Cells treated with 400 μM BPA showed increased pro–caspase 3 cleavage in a time-dependent manner, suggesting activation of caspase 3 (Fig. 4A,B). These findings suggest that BPA can induce cell death through apoptosis.

BPA-Induced ROS Production with Ca^{2+} Dependently

To study the effect of BPA on intracellular Ca^{2+}, we examined intracellular Ca^{2+} levels using a fluorescence microscope (Fig. 5A). Cells with increased intracellular Ca^{2+} displayed green fluorescence by Fluo-3/AM staining. We quantified the effect of BPA on the accumulation of intracellular Ca^{2+} using a fluorescence reader. We examined BPA treated with 400 μM at the indicated times (data not shown). BPA increased the level of intracellular Ca^{2+} after 20 min in a concentration-dependent manner. Pretreatment of cells with EGTA (1.5 mM), an extracellular Ca^{2+} chelator, blocked BPA-induced accumulation of Ca^{2+} (Fig. 5B).

Generation of ROS indicates oxidative stress, which can increase lipid peroxidation and induce cytotoxicity as a consequence. To examine the involvement of ROS in BPA-induced cytotoxicity, we measured the production of ROS using a fluorescent plate reader. BPA increased ROS production in a concentration-dependent manner (Fig. 6A). To investigate the relationship between intracellular Ca^{2+} and ROS, we treated cells with an extracellular Ca^{2+} chelator, EGTA (1.5 mM), and an intracellular Ca^{2+} chelator, BAPTA-AM (10 μM). Both inhibitors were added 30 min prior to the BPA treatment. Iron (100 μM $FeSO_4$) was used as a positive control for ROS generation. Both EGTA and BAPTA-AM significantly reduced BPA-induced ROS production (Fig. 6B). However, with BAPTA-AM pretreatment ROS production was reduced more than with

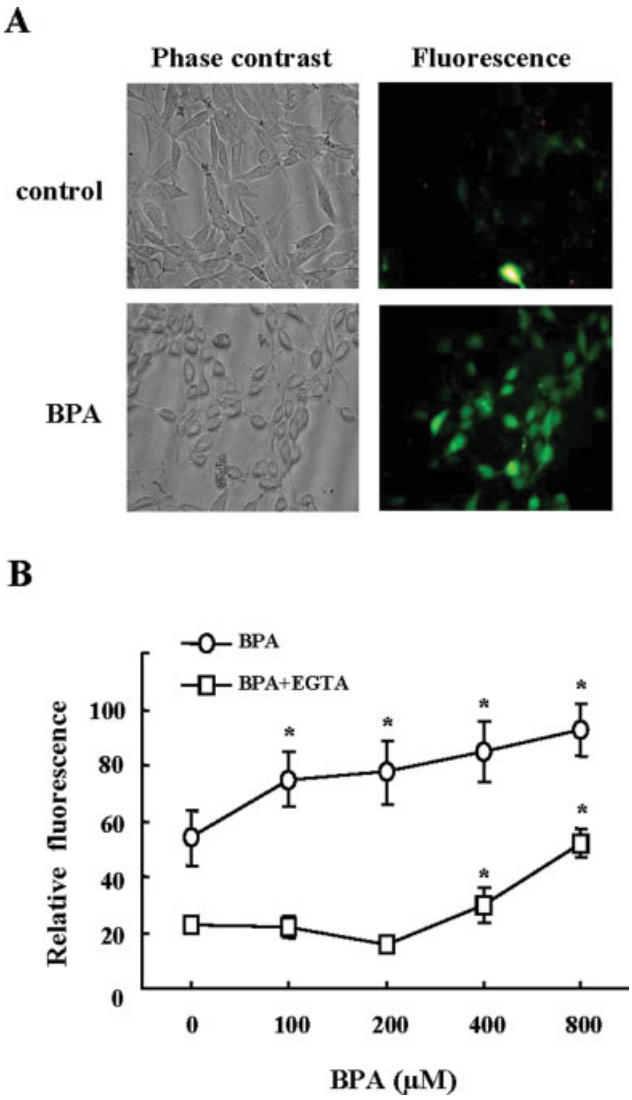

Fig. 5. Effects of BPA on intracellular calcium. Cells (2×10^4 cells/well in 96-well plates) were preincubated with Fluo-3/AM for 60 min. Fluo-3/AM was used to determine intracellular Ca^{2+}. **A:** Cells were treated with BPA 400 μM. After 20 min of treatment, fluorescent intensity was measured by a microscope for morphological and fluorescence change in cells. **B:** Cells were treated with BPA 400 μM or BPA plus EGTA (1.5 mM). After 20 min of treatment, fluorescent intensity was measured by a fluorescent plate reader. The results are presented as means ± SEMs of three independent experiments (⋆significantly different from the control). [Color figure can be viewed in the online issue, which is available at www.interscience.wiley.com.]

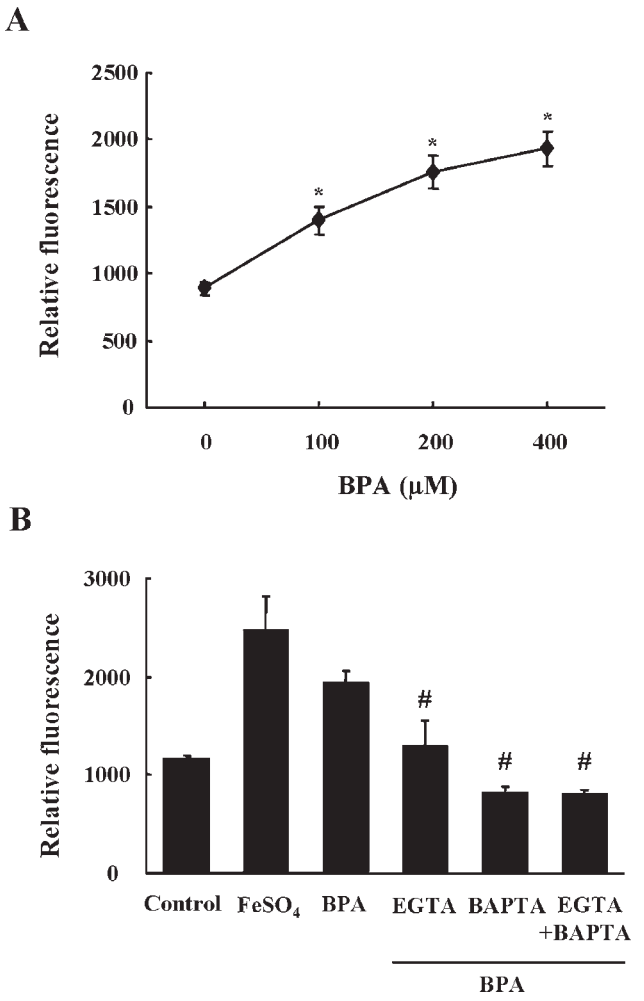

Fig. 6. Effects of BPA on ROS production. Cells (2×10^4 cells/well in 96-well plates) were stained with 10 μM of DHR for 30 min. Production of ROS was measured by DHR 123. **A:** Graph represents the fluorescence change after cells exposed to to various concentrations of BPA for 3 hr 30 min. **B:** All pharmacological agents (EGTA 1.5 mM, BAPTA 10 μM) were added 30 min before the BPA treatment. Iron (100 μM $FeSO_4$) was used as a positive control for ROS generation. After BPA treatment, DHR fluorescent intensity was recorded using a fluorescent plate reader. The results are presented as means ± SEMs of three independent experiments (⋆significantly different from the control; #significantly different from the BPA-treated value).

EGTA. In addition, there was no additive effect of the combination of EGTA and BAPTA-AM compared with using BAPTA-AM alone. There results suggest that BPA-induced ROS generation is regulated by intracellular Ca^{2+}.

BPA-induced Activation of MAPK and NF-κB

To determine the effect of BPA on activation of MAPKs, we studied the phosphorylation of three types of MAPKs: p38, ERK, and JNK (Fig. 7A,B). When a cell was treated with 400 μM BPA, phosphorylation of ERK and JNK peaked at 90 min and began to decrease toward control levels at 120 min. The phosphorylation of p38 was not altered by BPA (data not shown).

NF-κB controls the transcription of many signaling genes (Karin et al., 2002). Treatment with 400 μM BPA induced the degradation of IκBα and the nuclear translocation of p65 NF-κB after 1 hr of incubation, as

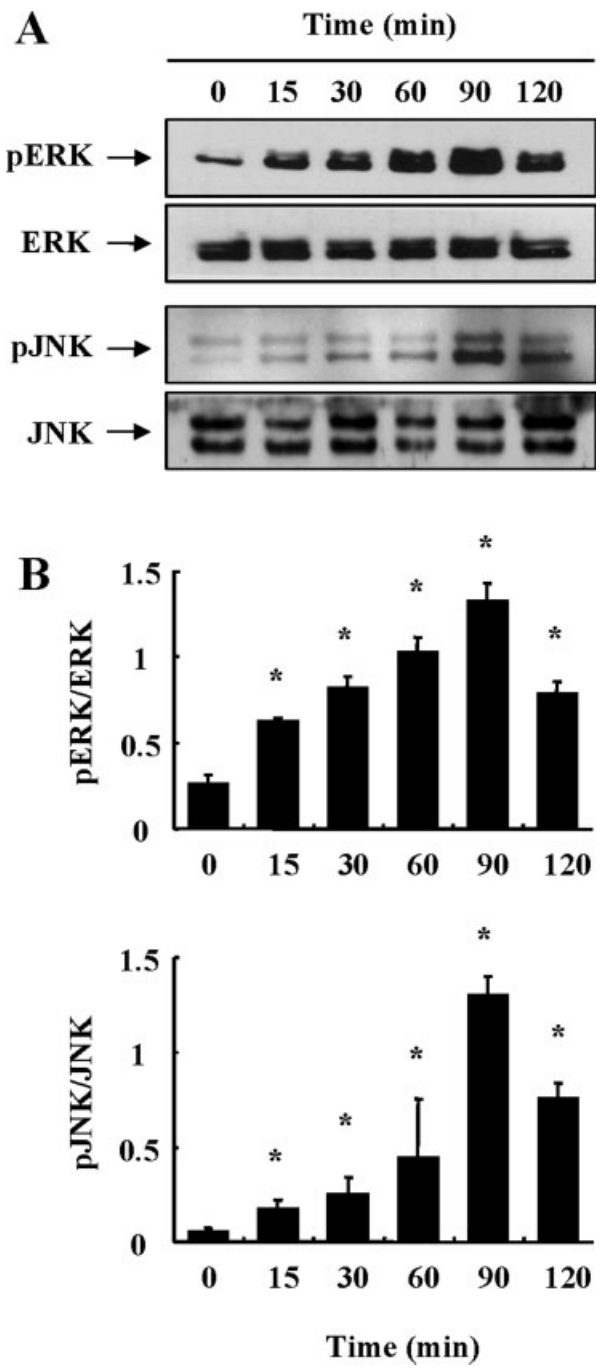

Fig. 7. Effects of BPA on MAPK activation. Cells (2×10^6 cells/well in 6-well plates) were stimulated with 400 μM of BPA at the indicated times. The phosphorylation of ERK and JNK was analyzed by Western blotting. **B:** Densitometric analysis of pERK and pJNK. Phosphorylation levels were normalized against total levels. The results are presented as means ± SEMs of three independent experiments (*significantly different from the control).

determined by Western blotting (Fig. 8A-C). To investigate whether NF-κB/DNA binding was caused by BPA, we employed EMSA (Fig. 8D,E). NF-κB/DNA binding peaked after 1 hr of BPA treatment and then decreased after 2 hr. PMA was used as a positive control. To further investigate the effect of BPA on NF-κB-dependent gene expression, the luciferase reporter gene assay was employed. HT-22 cells were transiently transfected with a plasmid containing NF-κB binding sites, and luciferase activity was measured. The luciferase activity in the BPA-treated group was increased almost 100-fold that in the untreated group (Fig. 8F). These results may indicate BPA-induced cell death through activation of MAPK and NF-κB.

BPA-induced Apoptotic Signal Pathway

To determine the roles of Ca^{2+}, ROS, ERK, JNK, and NF-κB in BPA-induced cell death, cells were treated with pharmacological inhibitors of ERK (10 μM PD98059), JNK (2.5 μM SP600125), NF-κB (25 μM PDTC), Ca^{2+} (10 μM BAPTA-AM), and antioxidant (2.5 mM NAC) 30 min prior to the BPA treatment (Kim and Sharma, 2004; Kim et al., 2007b). Cells were stained with Annexin V and analyzed using a flow cytometer. The apoptotic cells were significantly decreased when cells were pretreated with PD98059, SP600125, BAPTA-AM, and NAC before the BPA treatment (Fig. 9). These inhibitors have protective effects on BPA-induced apoptosis. Interestingly, the apoptotic cells were increased with pretreatment of PDTC 25 μM (Fig. 10A). To determine the possible cytotoxicity of PDTC, we tested the cytotoxicity of PDTC using the MTT assay (Fig. 10B). Although PDTC was not cytotoxic below 50 μM, the apoptotic cells were increased after cotreatment with BPA (400 μM) and PDTC (Fig. 10C). These data suggest that Ca^{2+}, ROS, ERK, and JNK play a role in BPA-induced apoptosis. In contrast, NF-κB suppressed BPA-induced apoptotic cell death.

DISCUSSION

The aims of our study were to determine the apoptotic effect of BPA and the mechanism of BPA-induced apoptosis in mouse hippocampal cells. To investigate the neurotoxicity of BPA, we employed 400 μM BPA based on our observation of cytotoxicity in hippocampal cells (Fig. 1). The concentration of BPA used in the present study was higher than normal environment exposure (BPA is 0.05 mg/kg/day, the reference dose in humans). However, BPA also has been found in indoor/outdoor air and floor dust, suggesting that humans could be exposed to this organic substance anywhere. Considering the various routes of exposure to BPA such as plastics, dental material, water, and air, 400 μM BPA (91.2 mg/mL) is a concentration that humans could realistically be exposed to in the environment (Tsai, 2006). Moreover, a 40 μg/kg dose of BPA can antagonize the action of estradiol in the adult rat hippocampus by blocking the stimulatory effect of estradiol on synaptogenesis (MacLusky et al., 2005). In some cases, BPA was cytotoxic to neural progenitor cells at a high concentration (>400 μM), and BPA decreased cell viability of PC-12 cells in a concentration-dependent manner (more than 50 μM) (Kim et al., 2007a;

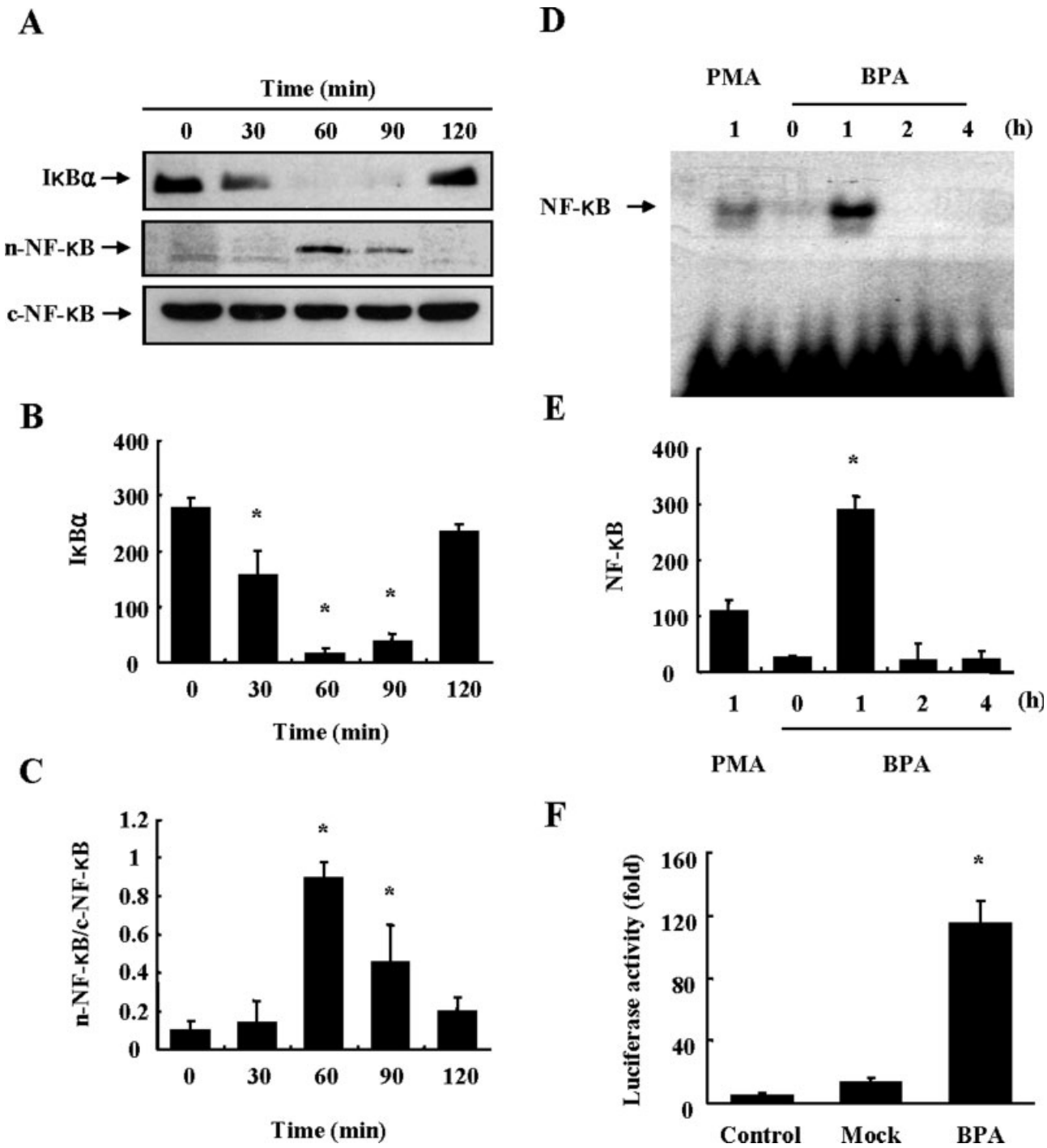

Fig. 8. Effects of BPA on NF-κB activation. **A:** Cells (2×10^6 cells/well in 6-well plates) were stimulated with 400 μM of BPA at the indicated times for NF-κB activation. The cell extract was analyzed by Western blotting for IκBα and nuclear translocation of NF-κB. **B:** Densitometric analysis of IκBα. **C:** Densitometric analysis of nuclear NF-κB. Nuclear translocation levels were normalized against cytoplasmic NF-κB levels. **D:** DNA binding activity of NF-κB. Cells were treated with PMA (40 nM, positive control) or BPA (400 μM). Nuclear extracts were isolated and used in an electrophoretic mobility shift assay with ^{32}P-labeled NF-κB oligonucleotide as a probe. **E:** Densitometric analysis of ^{32}P-labeled NF-κB. **F:** NF-κB-dependent luciferase gene expression. Cells (1×10^5 cells/well in 12-well plates) were transiently transfected with NF-κB luciferase reporter construct or empty vector. After 24 hr, the cells were treated with BPA 400 μM for 2 hr and harvested, and their luciferase activity was determined by a luciferase assay. Luciferase activity was expressed relative to the control (n-NF-κB, nuclear NF-κB; c-NF-κB, cytoplasmic NF-κB). The results are presented as means ± SEMs of three independent experiments (*significantly different from the control).

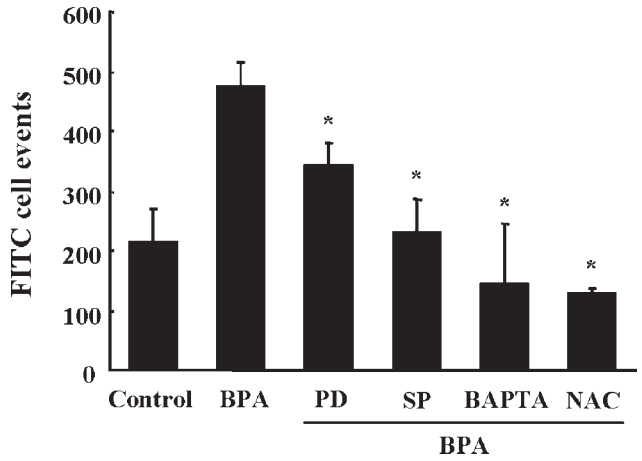

Fig. 9. Effects of pharmacological inhibitors on BPA-induced apoptosis. All pharmacological agents (10 μM PD 98059, 2.5 μM SP 600125, 10 μM BAPTA, 2.5 mM NAC) were added 30 min before the BPA treatment. Cells (2×10^5 cells/well in 12-well plates) were stained with Annexin V and analyzed using a flow cytometer. The results are presented as means ± SEMs of three independent experiments (*significantly different from the BPA-treated value).

Lee et al., 2007). Thus, we need to study the neurotoxicity of high doses of BPA as well as low doses. In our study, exposure of cells to BPA increased cell viability at low doses, which suggests that the low doses of BPA may induce protective effects. It was reported that a low concentration of BPA is neuroprotective against glutamate and amyloid beta in HT-22 cells (Gursoy et al., 2001). A low dose of BPA (less than 50 μM) may aid in the neurite extension of cells, resulting in cell protective effects that may be mediated by the estrogen receptor (Lee et al., 2007). These data suggest that BPA has a dose-differential effect on cell survival or cell death.

To investigate BPA-induced apoptotic cell death, we assayed BPA-induced morphological changes and observed time-dependent apoptotic cell death and nuclear condensation after BPA treatment. Our data indicate that BPA induces apoptotic cell death in hippocampal cells. When apoptosis is induced with an appropriate agent in cells, activation of caspase 3 is detected. Caspase 3 belongs to the cysteine protease family and is responsible for cleaving substrates such as DNA fragmentation factor that can go on to damage DNA and thus is considered an effector caspase (Sharif-Askari et al., 2001). Our data showed that caspase 3 was activated by BPA treatment.

Previous studies indicated that BPA decreases the viability of TM4 cells with elevation of the intracellular calcium level (Hughes et al., 2000). Increased intracellular Ca^{2+} induced ROS generation, a proapoptosis cascade (Hajnoczky et al., 2006). In fact, alteration of intracellular calcium concentration could be a significant contributor to the generation of ROS, thereby inhibiting cell survival. BPA induced ROS production and significantly compromised mitochondrial function concomitant with elevated expression and oxidization of DJ-1 (Ooe et al., 2005). BPA was found to induce the production of ROS in a concentration- and time-dependent manner in neural progenitor cells and human

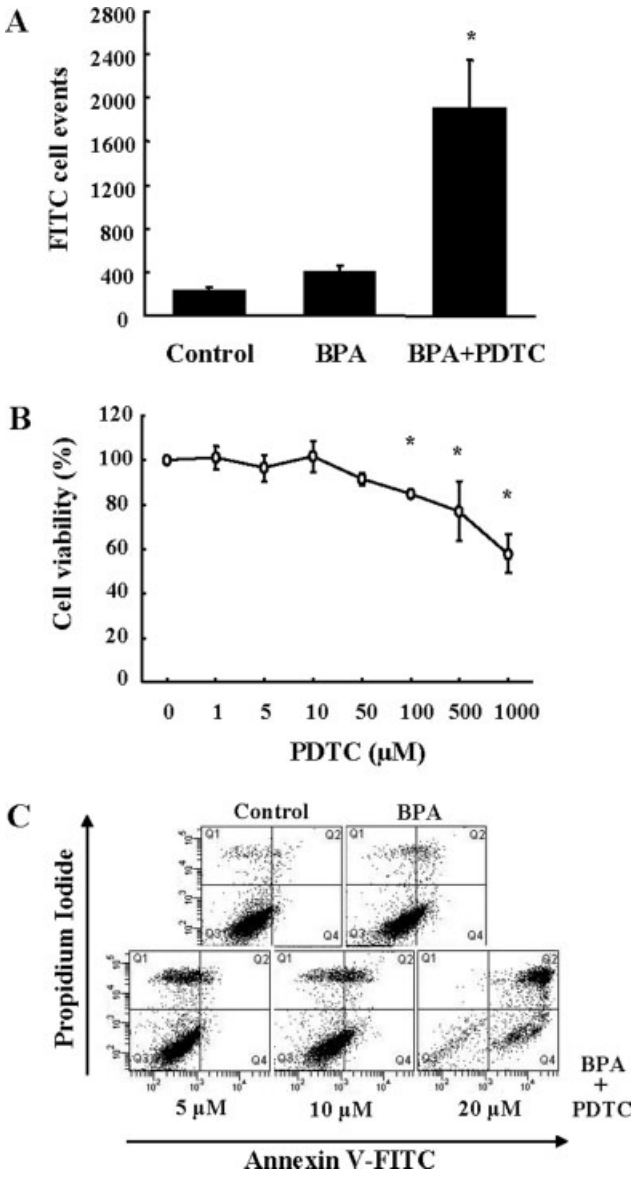

Fig. 10. Effects of PDTC on BPA-induced apoptosis. **A:** PDTC (25 μM) was added 30 min before the BPA treatment. Cells (2×10^5 cells/well in 12-well plates) were stained with Annexin V and analyzed using a flow cytometer. **B:** To indicate the effects of PDTC on cell viability, cells (2×10^4 cells/well in 96-well plates) were treated with various concentrations of PDTC for 24 hr. Cell viability was detected by the MTT assay. **C:** Various concentrations of PDTC were added 30 min before the BPA treatment. Cells (2×10^5 cells/well in 12-well plates) were stained with Annexin V and PI and were analyzed using a flow cytometer. A total of at least 1×10^4 cells were analyzed per sample. The results are presented as means ± SEMs of three independent experiments (*significantly different from the BPA-treated value).

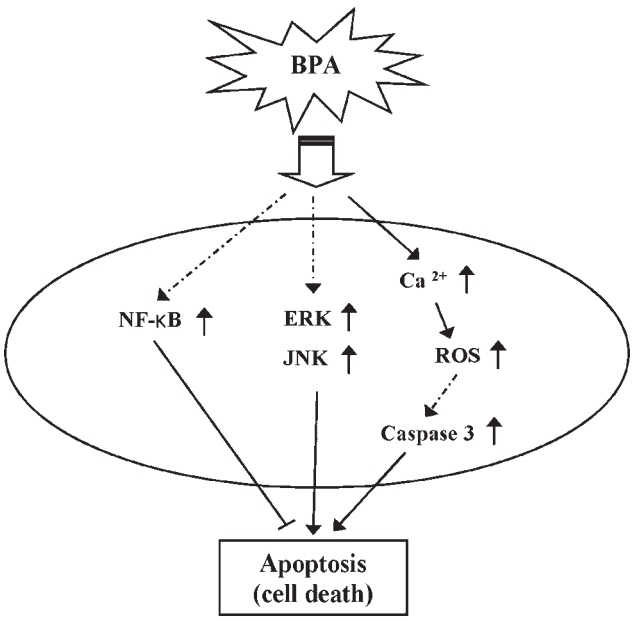

Fig. 11. Hypothetical mechanism on BPA-induced apoptosis in HT-22 cells. This schematic diagram showed that BPA-induced apoptosis is mediated by Ca^{2+}-activated ROS followed by caspase 3 activation, BPA-induced apoptosis by activation of ERK and JNK, but inhibited apoptosis by activation of NF-κB.

neutrophil granulocytes (Reistad et al., 2005; Kim et al., 2007a). Similarly, our experiments showed that intracellular Ca^{2+} accumulation was dose dependently increased by BPA. Levels of ROS were increased in a concentration-dependent manner in BPA-treated cells. To investigate the relation of intracellular Ca^{2+} with generation of ROS, we employed inhibitors of Ca^{2+}. Pretreatment of BAPTA-AM almost completely blocked BPA-induced ROS generation. These findings indicate that generation of ROS induced by BPA resulted from the increase of intracellular Ca^{2+}.

Some studies have shown that the MAPK family is activated depending on the cell type and nature of the stimuli in neuronal cell survival (Lee et al., 2007). Estrogen signaling may be initiated at either membrane or cytosolic location and can result in both direct local effects (such as modification of ion fluxes) and regulation of gene transcription secondary to activation of a kinase cascade, such as MAPKs (Driggers and Segars, 2002). Thus, diverse estrogenic compounds could activate MAPKs (Li et al., 2006). It was reported that BPA altered the activation of ERK and JNK in a different manner without affecting the activity of p38 (Kim et al., 2007a). Therefore, we tested the activation of MAPKs to determine whether these signals might be related to BPA-induced cell death. The results showed that BPA activated ERK and JNK, but not p38. This BPA-induced neurotoxic effect was prevented in the presence of ERK and JNK inhibitors. These results suggest that activation of the ERK and JNK pathway was involved in BPA-induced neuronal apoptosis.

NF-κB activates the transcription of several target genes that block the induction of apoptosis, as an inhibitor of programmed cell death (Karin et al., 2002). Some research has indicated that activation of NF-κB might protect cells from oxidative stress–induced neuronal cell death, suggesting that NF-κB activation may be an important signal for presenting cellular degeneration (O'Neill and Kaltschmidt, 1997). In our results, BPA induced apoptosis and stimulated the NF-κB signaling pathway. Activation of NF-κB was shown to inhibit apoptotic death of cells that initially suffered BPA-induced damage. As evidence, the cells pretreated with PDTC for inhibition of NF-κB had an increased apoptotic rate. Although the concentration of PDTC used in our experiments did not show cytotoxicity, PDTC induced apoptosis by inhibiting NF-κB activity. We speculated that NF-κB is activated for survival of signaling after BPA treatment at an early time but that at a later time, BPA induced apoptosis by activating ROS, MAPKs, and caspase 3 (Fig. 11).

In summary, BPA causes neuronal toxicity. This toxic effect may be mediated by calcium influx, generation of ROS, and activation of MAPK and caspase 3. In addition, BPA-activated NF-κB protects cells against BPA-induced cell death. Future studies are necessary to clarify the role of NF-κB and signaling mechanisms in BPA-induced apoptosis.

REFERENCES

Bindhumol V, Chitra KC, Mathur PP. 2003. Bisphenol A induces reactive oxygen species generation in the liver of male rats. Toxicology 188:117–124.

Buttke TM, Sandstrom PA. 1994. Oxidative stress as a mediator of apoptosis. Immunol Today 15:7–10.

Chitra KC, Latchoumycandane C, Mathur PP. 2003. Induction of oxidative stress by bisphenol A in the epididymal sperm of rats. Toxicology 185:119–127.

Driggers PH, Segars JH. 2002. Estrogen action and cytoplasmic signaling pathways. Part II: The role of growth factors and phosphorylation in estrogen signaling. Trends Endocrinol Metab 13:422–427.

Foehr ED, Bohuslav J, Chen LF, DeNoronha C, Geleziunas R, Lin X, O'Mahony A, Greene WC. 2000. The NF-kappa B-inducing kinase induces PC12 cell differentiation and prevents apoptosis. J Biol Chem 275:34021–34024.

Gursoy E, Cardounel A, Kalimi M. 2001. The environmental estrogenic compound bisphenol A exerts estrogenic effects on mouse hippocampal (HT-22) cells: neuroprotection against glutamate and amyloid beta protein toxicity. Neurochem Int 38:181–186.

Hajnoczky G, Csordas G, Das S, Garcia-Perez C, Saotome M, Sinha Roy S, Yi M. 2006. Mitochondrial calcium signalling and cell death: approaches for assessing the role of mitochondrial Ca2+ uptake in apoptosis. Cell Calcium 40:553–560.

Hao Y, Creson T, Zhang L, Li P, Du F, Yuan P, Gould TD, Manji HK, Chen G. 2004. Mood stabilizer valproate promotes ERK pathway-dependent cortical neuronal growth and neurogenesis. J Neurosci 24:6590–6599.

Hughes PJ, McLellan H, Lowes DA, Kahn SZ, Bilmen JG, Tovey SC, Godfrey RE, Michell RH, Kirk CJ, Michelangeli F. 2000. Estrogenic alkylphenols induce cell death by inhibiting testis endoplasmic reticulum Ca(2+) pumps. Biochem Biophys Res Commun 277:568–574.

Ichijo H, Nishida E, Irie K, ten Dijke P, Saitoh M, Moriguchi T, Takagi M, Matsumoto K, Miyazono K, Gotoh Y. 1997. Induction of apoptosis by ASK1, a mammalian MAPKKK that activates SAPK/JNK and p38 signaling pathways. Science 275:90–94.

Kabuto H, Hasuike S, Minagawa N, Shishibori T. 2003. Effects of bisphenol A on the metabolisms of active oxygen species in mouse tissues. Environ Res 93:31–35.

Karin M, Cao Y, Greten FR, Li ZW. 2002. NF-kappaB in cancer: from innocent bystander to major culprit. Nat Rev Cancer 2:301–310.

Kim K, Son TG, Kim SJ, Kim HS, Kim TS, Han SY, Lee J. 2007a. Suppressive effects of bisphenol A on the proliferation of neural progenitor cells. J Toxicol Environ Health A 70:1288–1295.

Kim SH, Johnson VJ, Sharma RP. 2002. Mercury inhibits nitric oxide production but activates proinflammatory cytokine expression in murine macrophage: differential modulation of NF-kappaB and p38 MAPK signaling pathways. Nitric Oxide 7:67–74.

Kim SH, Lee S, Suk K, Bark H, Jun CD, Kim DK, Choi CH, Yoshimura T. 2007b. Discoidin domain receptor 1 mediates collagen-induced nitric oxide production in J774A.1 murine macrophages. Free Radic Biol Med 42:343–352.

Kim SH, Sharma RP. 2004. Mercury-induced apoptosis and necrosis in murine macrophages: role of calcium-induced reactive oxygen species and p38 mitogen-activated protein kinase signaling. Toxicol Appl Pharmacol 196:47–57.

Lee YM, Seong MJ, Lee JW, Lee YK, Kim TM, Nam SY, Kim DJ, Yun YW, Kim TS, Han SY, Hong JT. 2007. Estrogen receptor independent neurotoxic mechanism of bisphenol A, an environmental estrogen. J Vet Sci 8:27–38.

Li X, Zhang S, Safe S. 2006. Activation of kinase pathways in MCF-7 cells by 17beta-estradiol and structurally diverse estrogenic compounds. J Steroid Biochem Mol Biol 98:122–132.

MacLusky NJ, Hajszan T, Leranth C. 2005. The environmental estrogen bisphenol a inhibits estradiol-induced hippocampal synaptogenesis. Environ Health Perspect 113:675–679.

Oka T, Adati N, Shinkai T, Sakuma K, Nishimura T, Kurose K. 2003. Bisphenol A induces apoptosis in central neural cells during early development of Xenopus laevis. Biochem Biophys Res Commun 312:877–882.

O'Neill LA, Kaltschmidt C. 1997. NF-kappa B: a crucial transcription factor for glial and neuronal cell function. Trends Neurosci 20:252–258.

Ooe H, Taira T, Iguchi-Ariga SM, Ariga H. 2005. Induction of reactive oxygen species by bisphenol A and abrogation of bisphenol A–induced cell injury by DJ-1. Toxicol Sci 88:114–126.

Pande V, Ramos MJ. 2005. NF-kappaB in human disease: current inhibitors and prospects for de novo structure based design of inhibitors. Curr Med Chem 12:357–374.

Purves T, Middlemas A, Agthong S, Jude EB, Boulton AJ, Fernyhough P, Tomlinson DR. 2001. A role for mitogen-activated protein kinases in the etiology of diabetic neuropathy. Faseb J 15:2508–2514.

Reistad T, Mariussen E, Fonnum F. 2005. The effect of a brominated flame retardant, tetrabromobisphenol-A, on free radical formation in human neutrophil granulocytes: the involvement of the MAP kinase pathway and protein kinase C. Toxicol Sci 83:89–100.

Sakon S, Xue X, Takekawa M, Sasazuki T, Okazaki T, Kojima Y, Piao JH, Yagita H, Okumura K, Doi T, Nakano H. 2003. NF-kappaB inhibits TNF-induced accumulation of ROS that mediate prolonged MAPK activation and necrotic cell death. Embo J 22:3898–3909.

Seo SR, Chong SA, Lee SI, Sung JY, Ahn YS, Chung KC, Seo JT. 2001. Zn2+-induced ERK activation mediated by reactive oxygen species causes cell death in differentiated PC12 cells. J Neurochem 78:600–610.

Sharif-Askari E, Alam A, Rheaume E, Beresford PJ, Scotto C, Sharma K, Lee D, DeWolf WE, Nuttall ME, Lieberman J, Sekaly RP. 2001. Direct cleavage of the human DNA fragmentation factor-45 by granzyme B induces caspase-activated DNase release and DNA fragmentation. Embo J 20:3101–3113.

Staples CA, Dorn PB, Klecka GM, O'Block ST, Harris LR. 1998. A review of the environmental fate, effects, and exposures of bisphenol A. Chemosphere 36:2149–2173.

Tsai WT. 2006. Human health risk on environmental exposure to bisphenol-A: a review. J Environ Sci Health C Environ Carcinog Ecotoxicol Rev 24:225–255.